UDK 539.3

S.M. Vereshaka, Dr. tehn. sciences, prof., Sumy state univ.,
Riadh Abdulah ALAlaf, master, Mosul univ., Iraq,
Emad Toma Karash, master, Sumy state univ.

BUNDE STRESS THEORY OF SEMICIRCULAR LAYERED COMPOSITE CURVED BARS

С.М. Верещака, Ріяді Абдулла Алалаф, Імад Тома Караш. **Багатошарова теорія напружень розшарування напівкруглих шаруватих криволінійних стержнів з композитних матеріалів.** Використовуючи анізотропну теорію пружності, розраховано напруження у напівкруглих пластинчастих змішаних вигнутих брусках, підданих дії кінцевих сил і кінцевих згинальних моментів, визначено їх радіальні положення. Представлено сім'ю креслень кривих, показано зміну інтенсивності напружень та їх радіальних положень за різної геометрії і рівнів анізотропії напівкруглих кривих. Вплив анізотропії на положенні піків розшарування напруження визначено як малий. Використано програмний пакет MathCAD 14 для отримання максимально точних результатів.

Ключові слова: напружений стан, композитний вигнутий брусок напівкруглої форми, кінцеве зусилля, кінцевий згинальний момент.

С.М. Верещака, Рияде Абдулла Алалаф, Имад Тома Караш. **Многослойная теория напряжений расслоения полукруглых слоистых криволинейных стержней из композитных материалов.** Используя анизотропную теорию упругости, рассчитаны напряжения в полукруглых пластинчатых смешанных изогнутых брусках, подвергнутых воздействию конечных сил и конечных изгибающих моментов, определены их радиальные положения. Представлено семейство чертежей кривых, показано изменение интенсивности напряжений и их радиальных положений с различными геометрией и уровнями анизотропии полукруглых кривых. Влияние анизотропии на положение пиков, расслаивающих напряжение, определено как слабое. Использован программный пакет MathCAD 14 для получения наиболее точных результатов.

Ключевые слова: напряженное состояние, композитный полукруглый изогнутый брусок, конечное усилие, конечный изгибающий момент.

S.M. Vereshaka, Riadh Abdulah ALAlaf, Emad Toma Karash. **Bunde stress theory of semicircular layered composite curved bars.** Using anisotropic elasticity theory, stresses in a semicircular laminated composite curved bar subjected to finite/end forces and finite/end moments are calculated, and their radial locations are determined. A family of design curves is presented, showing variation of the intensity of stresses and their radial locations with different geometry and different degrees of anisotropy of the semicircular curves. The effect of value change in tangential coordinate caused change in location and value of maximum radial stress, tangential stress and shear stress. The effect of anisotropy on the location of peak delamination stress is found to be small. The Math CAD-14 program has been used to get most accurate results.

Keywords: stress state, a semicircular composite curved bar, finite/end force, finite bending moment.

Introduction

The applications of composite materials in high gas cylinder, pipes and other engineering structures are ever increasing, due to their highly desirable properties like high specific strength/ stiffness, low co-efficient of expansion, damping properties and directional dependence [1...4]. The problem of elastic equilibrium of an inhomogeneous cylinder by the force and torque is similar to the problem of bending of a semicircular curve bar moments and the force acting in the median plane. In the design and analysis of laminated composite cylinders, axis symmetric loads and ax symmetric geometries are often assumed for developing closed-form analytic solutions. In addition, the cylinder is assumed to have an infinite length such that the stresses are not only independent of the circumferential coordinate but also independent of the axial coordinate [5].

Solutions have been formulated on the basis of both the anisotropic elasticity theory and the la-

ISSN 2076-2429 (print)
ISSN 2223-3814 (on line)

minated shell theory. The laminated shell theory provides an accurate solution for thin-walled cylinders, whereas elasticity solutions are required for an accurate determination of the three-dimensional stress states that exist in thick-walled cylinders. In both of these analytical approaches, further simplifications are obtained by restricting the composite cylinder to be orthotropic [6...8].

The purpose of this paper is to represent documentarily the calculation of stress state in semicircular composite bar and its exact radial location, maximum stress as well as to describe how stress and its location change with the changes in degree of anisotropy and the wall thickness of the curved bar.

Composite curved bar

Figure 1 shows a semicircular composite curved bar of hollow cylinder subjected to end forces *P*, both ends of the curved bar being extended slightly. Thus, the loading axis will have slight offset *e* from the vertical diameter of the curved bar. Therefore, the loading state in figure 1 is the combination of two cases:

Bending due to end forces *P* with the loading axis coinciding with the vertical diameter of the curved bar.

Pure bending due to end moments *M* (=*Pe*) created by the loading axis offset *e.*

It has been observed that the highest probability of examined effect onset takes place at the interfaces of 0° and 90° plies because of high Poisson's ratio mismatch [9]. In constructing the curved bar test coupon, it is desirable to introduce 90° plies at, or in the vicinity of, a peak stress point (that is, a peak radial tensile stress point or peak shear stress point) and thereby ensure that the delamination will initiate at the peak stress point, which is yet to be determined. In the following sections, the peak radial tensile stress (or peak shear stress) and it's radial. Location will be calculated.

1. Anisotropic curved bar under end force

Figure 2 shows the anisotropic semicircular curved bar subjected to end forces P with the loading axis coinciding with the vertical diameter of the curved bar.

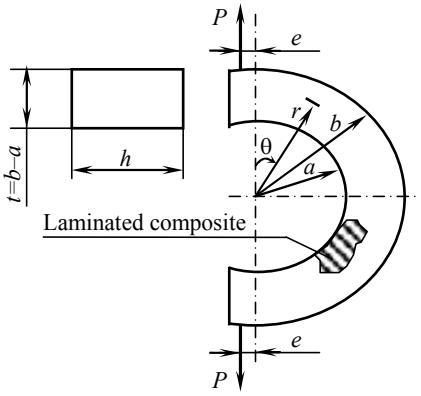

Fig. 1. Laminated composite semicircular curve bar test coupon for delamination study

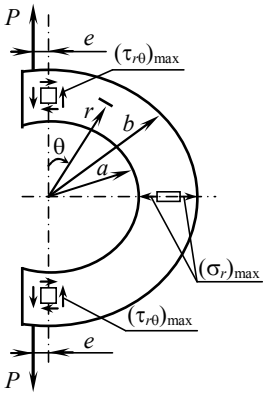

Fig. 2. Bending of semicircular curve bar by forces at its ends

Stresses induced

If the composite material of the curved bar is treated as a continuous anisotropic material, then the stresses induced in the composite curved bar due to the end forces *P* may be written as [5].

$$\sigma_r(r,\theta) = \frac{P}{bhg_1}\frac{b}{r}\left[\left(\frac{r}{b}\right)^{\beta} + \left(\frac{a}{b}\right)^{\beta}\left(\frac{b}{r}\right)^{\beta} - 1 - \left(\frac{a}{r}\right)^{\beta}\right]\sin\theta; \quad (1)$$

$$\sigma_\theta(r,\theta) = \frac{P}{bhg_1}\frac{b}{r}\left[(1-\beta)\left(\frac{r}{b}\right)^{\beta} + (1-\beta)\left(\frac{a}{b}\right)^{\beta}\left(\frac{b}{r}\right)^{\beta} - 1 - \left(\frac{a}{b}\right)^{\beta}\right]\sin\theta; \quad (2)$$

$$\tau_{r\theta}(r,\theta)=\frac{P}{bhg_1}\frac{b}{r}\left[\left(\frac{r}{b}\right)^{\beta}+\left(\frac{a}{b}\right)^{\beta}\left(\frac{b}{r}\right)^{\beta}-1-\left(\frac{a}{b}\right)^{\beta}\right]\cos\theta, \tag{3}$$

where: a is the curved bar inner radius, the b represents the curved bar outer radius, and h the width of the curved bar, r radial coordinate, θ tangential coordinate, σ_r radial stress, σ_θ tangential stress, $\tau_{r\theta}$ shear stress, and

$$g_1=\left[\frac{2}{\beta}1-\left(\frac{a}{b}\right)^{\beta}\right]+\left[1+\left(\frac{a}{b}\right)^{\beta}\ln\frac{a}{b}\right]. \tag{4}$$

And the anisotropic parameter β is defined as

$$\beta=\sqrt{1+\frac{E_\theta}{E_r}(1-2\nu_{\theta r})+\frac{E_\theta}{E_r}}, \tag{5}$$

where: E_θ is the modulus of elasticity in θ direction, E is the modulus of elasticity in r direction, $G_{\theta r}$ Shear modulus, and $\nu_{\theta r}$ Poisson's ratio. For isotropic materials, $\beta=2$.

Consequently to equations (1) and (3) the magnitudes of σ and are identical, but they are out of phase by. $\pi/2$ The maximum value of σ occurs at cross section $\theta=\pi/2$, and $\tau_{r\theta}$ reaches its peak value at the two load application cross sections ($\theta=0$) and ($\theta=\pi$):

$$\sigma_r\left(r,\frac{\pi}{2}\right)=-\tau_{r\theta}(\upsilon,0)=\tau_{r\theta}(r,\pi). \tag{6}$$

Thus, the semicircular curved-bar test coupon can provide the same intensities of open-mode and shear mode delamination stresses simultaneously. If the composite is weak in open-mode strength, the delamination will initiate at the midspan ($\theta=\pi/2$). On the other hand, if the composite is weak in shear strength, delamination will start at both ends of the curved bar (that is, ($\theta=0$) and ($\theta=\pi$) [9] :

Because of the relationship between σ and $\tau_{r\theta}$ given in equation (6), analysis will be limited to σ.

Equation (1) (for $\theta=\pi/2$) may be rewritten as:

$$\sigma_r\left(r,\frac{\pi}{2}\right)=\frac{P}{bh\,B}\frac{a}{r}\left[\left(\frac{r}{b}\right)^{\beta}+\left(\frac{b}{a}\right)^{\beta}\left(\frac{a}{r}\right)^{\beta}-1-\left(\frac{b}{a}\right)^{\beta}-1\right], \tag{7}$$

where

$$B=\frac{2}{\beta}\left[\left(\frac{a}{b}\right)^{\beta}-1\right]-\left[\left(\frac{a}{b}\right)^{\beta}+1\right]\ln\frac{a}{b}. \tag{8}$$

Location of maximum

The radial location $r=r_m$ where $\sigma_r(\rho,\ \pi/2)$ reaches its peak value $(\sigma_r)_{\max.}$ may be found by differentiating equation (7) with respect to ρ and setting the resulting derivative to zero, or

$$\frac{d}{dr}\left[\sigma_r\left(r,\frac{\pi}{2}\right)\right]=0. \tag{9}$$

From which it is found as

$$\left(\frac{r_m}{a}\right)^{\beta}=\frac{1}{2(\beta-1)}\left\{\sqrt{\left[\left(\frac{b}{a}\right)^{\beta}+1\right]^2+a(\beta^2-1)\left(\frac{b}{a}\right)^{\beta}}-\left[\left(\frac{b}{a}\right)^{\beta}+1\right]\right\}. \tag{10}$$

May be written as $(\sigma_r)_{\max}$

ISSN 2076-2429 (print)
ISSN 2223-3814 (on line)

$$(\sigma_r)_{\max.} = \sigma_r\left(r_m, \frac{\pi}{2}\right) = \frac{P}{(b-a)hB}\frac{a}{r_m}\left[\left(\frac{r_m}{b}\right)^{\beta} + \left(\frac{b}{a}\right)^{\beta}\left(\frac{a}{r_m}\right)^{\beta} - 1 - \left(\frac{b}{a}\right)^{\beta} - 1\right], \quad (11)$$

where r_m is given by equation (10).

2. Anisotropic curved bar under end bending moments.

Figure 3 shows the anisotropic curved bar under pure bending due to moment M.

Stress induced

When the composite material of the curved bar is treated as continuous material, the radial stress tangential stress, and shear stress induced in the curved bar under the end moments M would be expressed as [5]

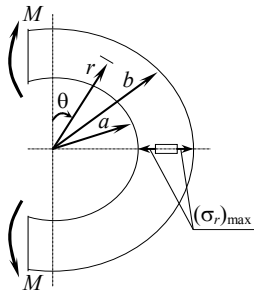

Fig. 3. Bending of semicircular curved of curved bar by moments at its ends

$$\sigma'_r(r) = -\frac{M}{b^2 hg}\left[1 - \frac{1-(a/b)^{k+1}}{1-(a/b)^{2k}}\left(\frac{r}{b}\right)^{k-1} - \frac{1-(a/b)^{k-1}}{1-(a/b)^{2k}}\left(\frac{a}{b}\right)^{k+1}\left[\frac{b}{r}\right]^{k+1}\right]; \quad (12)$$

$$\sigma'_\theta(r) = -\frac{M}{b^2 hg}\left[1 - \frac{1-(a/b)^{k+1}}{1-(a/b)^{2k}}k\left(\frac{r}{b}\right)^{k-1} + \frac{1-(a/b)^{k-1}}{1-(a/b)^{2k}}k\left(\frac{a}{b}\right)^{k+1}\left(\frac{b}{r}\right)^{k+1}\right]; \quad (13)$$

$$\tau'_{r\theta} = 0,$$

where the anisotropic parameter k is defined by:

$$k = \sqrt{\frac{E_\theta}{E_r}} \quad (15)$$

and

$$g = \frac{1-(a/b)^2}{2} - \frac{k}{k+1}\frac{[1-(a/b)^{k+1}]^2}{[1-(a/b)^{2k}]} + \frac{k(a/b)^2}{k-1}\frac{[1-(a/b)^{k-1}]^2}{[1-(a/b)^{2k}]} \quad (16)$$

Location of maximum stress

Differentiating equation (13) with respect to r, and setting the resulting derivative to zero,

$$\frac{d}{dr}[\sigma'_r(r)] = 0. \quad (17)$$

The radial location r'_m of the maximum σ'_m may be calculated as:

$$\left(\frac{r'_m}{a}\right)^{2k} = \frac{(k+1)(b/a)^{k+1}[(a/b)^{k-1}-1]}{(k-1)[(b/a)^{k+1}-1]}. \quad (18)$$

For the isotropic case ($k \to 1$), equation (18) is reduced to

$$\left(\frac{r'_m}{a}\right)_{k\to 1} = \frac{b}{a}\sqrt{\frac{2\ln b/a}{(b/a)^2 - 1}}, \quad (19)$$

where the relationship

$$\left\{\frac{[(b/a)^{k-1}-1]}{k-1}\right\}_{k\to 1} = \frac{\ln(b/a)^{k-1}}{k-1} = \ln\frac{b}{a}, \quad (20)$$

has been applied.

$$\frac{ha_m(b-a)}{M}(\sigma'_r)_{\max} = -\frac{(b/a)^2-1}{2C} \times$$
$$\times\left\{\left[\left(\frac{b}{a}\right)^{2k} - 1\right] - \left[\left(\frac{b}{a}\right)^{k+1} - 1\right]\left(\frac{r'_m}{a}\right)^{k-1} - \left[\left(\frac{b}{a}\right)^{k-1} - 1\right]\left(\frac{b}{a}\right)^{k+1}\left(\frac{r'_m}{a}\right)^{-(k+1)}\right\}, \quad (21)$$

where r'_m is given in equation (18).

Maximum stress

The open-mode maximum stress σ_D induced in the curved bar under the end force P with the loading axis offset e (see figure 1) will be the sum of $(\sigma_r)_{\max}$ Due to P without loading axis offset c (equation (10)) and $(\sigma')_{\max}$ due to ($M=Pe$) (equation (21), see figure 3):

$$\sigma_D = (\sigma_r)_{\max} + (\sigma'_r)_{\max} = \frac{P}{h(b-a)}\left[F_1 + F_2\frac{e}{a_m}\right], \tag{22}$$

where

$$F_1 = \frac{1}{B}\left(\frac{b}{a}-1\right)\frac{a}{r_m}\left[\left(\frac{r_m}{a}\right)^{\beta} + \left(\frac{b}{a}\right)^{\beta}\left(\frac{a}{r_m}\right)^{\beta} - \left(\frac{b}{a}\right) - 1\right];$$

$$F_2 = \frac{1}{2C}\left[\left(\frac{b}{a}\right)^2 - 1\right]\left\{\left[\left(\frac{b}{a}\right)^{2k} - 1\right] - \left[\left(\frac{b}{a}\right)^{k+1} - 1\right]\left(\frac{r'_m}{a}\right)^{k-1}\right\}; \tag{23}$$

$$a_m = \frac{a+b}{2}.$$

For thin-walled curved bar, the values of F1 and F2 are quite close, or

$$F_1 \approx F_2. \tag{24}$$

Therefore, the stress contribution from the end moment [Pe] for the thin-walled curved bar is almost proportional at the value of e/a_m.

Numerical results

To extract the results, the MATHCAT-14 program has been used. The curved bar is made of 31 composite plies and with the following plies properties: $[0_2^\circ/90^\circ/0_2^\circ/\pm45^\circ/(0_2^\circ/90)_2/\pm45^\circ/\overline{0}^\circ]_S$ With the stacking code

$$E_L = 17,24\cdot10^6\ \text{N/mm}^2,\quad E_T = 0,83\cdot10^6\ \text{N/mm}^2,$$
$$G_L = 0,41\cdot10^6\ \text{N/mm}^2,\quad \nu_{LT} = 0,33,\quad \nu_{TL} = 0,015,$$

$$E_L = 17,24\cdot10^6\ \text{N/mm}^2,\quad E_T = 0,83\cdot10^6\ \text{N/mm}^2,$$
$$G_L = 0,41\cdot10^6\ \text{N/mm}^2,\quad \nu_{LT} = 0,33,\quad \nu_{TL} = 0,015$$

and forces (P=20 KN), dimension hollow cylinder [a=100 mm, b=109 mm, e=40 mm, h=25 mm, ω=0°, ω is angle forces, δ=0,015, δ is composite ply thickness, ψ_1=0,55, ψ_3=0,01, r=100…109 mm, θ=0°, 90°, 180°]. ψ_1, ψ_3 are the relative volume content reinforcement layer in the direction of axes (1) and (3).The following elastic tensile and shear properties obtained using program MATHCAT14.

$$E_\theta = 8,263\cdot10^6\ \text{N/mm}^2,\quad E_r = 5,668\cdot10^6\ \text{N/mm}^2,\quad E_z = 3,14\cdot10^6\ \text{N/mm}^2,$$
$$G_{r\theta} = 0,804\cdot10^6\ \text{N/mm}^2,\quad G_{rz} = 0,095\cdot10^6\ \text{N/mm}^2,\quad G_{\theta z} = 0,084\cdot10^6\ \text{N/mm}^2,$$
$$\nu_{r\theta} = 0,181,\quad \nu_{rz} = 0,018,\quad \upsilon_{\theta z} = 0,017.$$

From table 1. Realized is the following: when (θ=0°, 90°), the value of (σ_r=σ_θ=0) but value $\tau_{r\theta}$ was maximum when the (r_m=104,38 mm) stress value ($\tau_{r\theta}$=133,4 MPa). This does mean that when applied vertical forces P on a curved semi-circular curved bar, the maximum stress was $\tau_{r\theta}$. But when the value of (θ=90°) we note that the value ($\tau_{r\theta}$=0) and the highest value of stress $(\sigma_r)_{\max}$ was when (r=r_m=104,38 mm) and the value of stress ($(\sigma_r)_{\max}$=133,4 MPa) the highest value σ_θ)was when (r=a) it is equal to (σ_θ=6470 MPa). Also from figure 1. we note that the value of σ_r when (r=a) was zero and

ISSN 2076-2429 (print)
ISSN 2223-3814 (on line)

increases with increasing the value of r and reaches the highest value when the ($r=r_m$=104,38 mm) it is equal to (σ_r=133,4 MPa) and then start the value of stress after this point decrease until it reaches zero when the ($r=b$). Figure 5 shows when (θ=0) the value ($\tau_{r\theta}$=0) and increases with increasing r until it reaches the highest value when (r_m=104,38 mm) maximum stress ($\tau_{r\theta}$=133.4 MPa), but after this point begins the downward increase in the value of r until it reaches zero when ($r=b$), as well as the same case when (θ=180°) but the values are negative (compression stress) and the values appear opposite in figure. Figure 6 shows when (θ=90°) the value of σ_θ was the highest value when ($r=a$) it is equal to (σ_θ=6473 MPa), but begin a downward until it reaches the value of stress (σ_θ=0) when (r_m=104,5 mm) and then begin to increase (compression stress) until it reaches the highest value when ($r=b$) it is equal to (σ_θ=5939 MPa).

Table 1

Shows r as function of stresses for different values of θ when applied forces on the ends

θ =180°			θ=90°			θ=0°			r, mm	№
$\tau_{r\theta}$, MPa	σ_θ, MPa	σ_r, MPa	$\tau_{r\theta}$, MPa	σ_θ, MPa	σ_r, MPa	$\tau_{r\theta}$, MPa	σ_θ, MPa	σ_r, MPa		
0	0	0	0	6473	0	0	0	0	100	1
–56,35	0	0	0	4978	56,35	56,35	0	0	101	2
–96,66	0	0	0	3517	96,66	96,66	0	0	102	3
–121,85	0	0	0	2088	121,85	121,85	0	0	103	4
132,78	0	0	0	690	132,78	132,78	0	0	104	5
–130,26	0	0	0	–682	130,26	130,26	0	0	105	6
–115,05	0	0	0	–2029	115,05	115,05	0	0	106	7
–87,84	0	0	0	–3354	87,84	87,84	0	0	107	8
49,29	0	0	0	–4655	49,29	49,29	0	0	108	9
0	0	0	0	–5939	0	0	0	0	109	10

From table 2 when we applied moment M on semicircular curved bar it is evident that when the value of (θ=0°, 180°), the value of stresses ($\sigma'=\tau_{r\theta}$=0) but maximum stress σ'_θ and from the table we note that it be fixed and not depend on changing the value of r and the value is equal to (σ_θ=2441 MPa). But when the value of (θ=90°), the value of stress ($\tau_{r\theta}$=0) but the highest value of stress σ' is when ($r=r'_m$=104,34 mm) and the amount equal to (σ'=51,09 MPa) and the lowest value is when ($r=a$, $r=b$). The highest value of stress σ'_θ is when ($r=a$) and value (σ'_θ=2441 MPa) and less than the value of the stress increase in the value of r until it reaches its minimum when (r=104,38 mm) and value (σ'_θ=230 MPa). From eqution (26) maximum stress σ_D under the end forces P and moment M equal ($\sigma_D=(\sigma_r)_{max}+(\sigma')_{max}$=184,49 MPa) and ($\sigma_D=(\sigma_\theta)_{max}+(\sigma'_\theta)_{max}$=8911 MPa).

Also by using MATHCAT-14 was obtained the following results: From the figure 4 shows the dimensionless de1amination stress $[h(b–a)/P](\sigma_r)_{max}$ induced by the end forces P plotted as a function of b/a for different values of anisotropic parameter β. As $b\to a$, the effect of anisotropy disappeared, and all the curves converge into a single point giving $[h(b–a)/P](\sigma_r)_{max}$=1,5, which has been established in equation (11). For low anisotropy $2\le\beta\le5$, the delamination stress increases monotonically with the increase of b/a. However, for high anisotropy of $\beta>5$, the de1amination stress curves show a slight valley (or dent) in the regions of moderate values of b/a. In these regions $[h(b–a)/P](\sigma_r)_{max}$ yields values less than 1,5. Notice that as the value of β increases, the intensity of de1amination stress decreases, and that the higher the value of b/a (that is, the thicker the wall), the higher the magnitude of the delamination stress.

Table 2

Shows r'_m as function of stresses for different values of θ when applied moment on the ends

θ=180°			θ=90°			θ=0°			r, mm	№
$\tau_{r\theta}$, MPa	σ_θ, MPa	σ_r, MPa	$\tau_{r\theta}$, MPa	σ_θ, MPa	σ_r, MPa	$\tau_{r\theta}$, MPa	σ_θ, MPa	σ_r, MPa		
0	2241	0	0	2441	0	0	2241	0	100	1
0	2241	0	0	1871	21,34	0	2241	0	101	2
0	2241	0	0	1313	36,73	0	2241	0	102	3
0	2241	0	0	767	46,46	0	2241	0	103	4
0	2241	0	0	230	50,80	0	2241	0	104	5
0	2241	0	0	–296	49,99	0	2241	0	105	6
0	2241	0	0	–812	44,29	0	2241	0	106	7
0	2241	0	0	–1319	33,91	0	2241	0	107	8
0	2241	0	0	–1816	19,08	0	2241	0	108	9
0	2241	0	0	–2304	0	0	2241	0	109	10

Figure 5 shows the dimensionless radial distance $[(r_m/a)–1]/[(b/a)–1]$ of $(\sigma_r)_{max}$ point measured from the inner boundary of the curved bar plotted as a function of b/a. It is seen that the effect of anisotropy is relatively small and is negligible in the region $b/a<1,4$. As the value of b/a increases, the location of $(\sigma_r)_{max}$ moves away from the middle surface and toward the inner boundary of the curved bar.

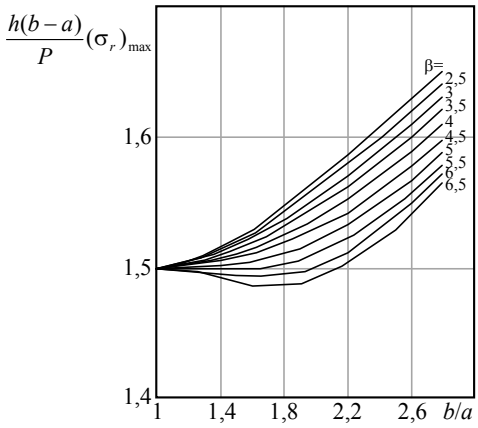

Fig. 4. Plots of delamination stress $(\sigma r)_{max}$ As function of a/b for different valves of β

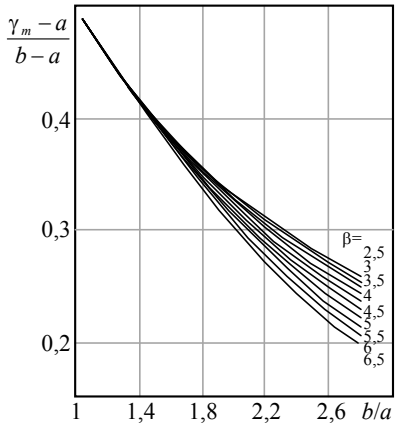

Fig. 5. Plots of location of stress $(\sigma r)_{max}$ As function of a/b for different valves of β

Figure 6 shows the plots of the dimensionless delamination stress $h(b–a)/M](\sigma_r)_{max}$ induced by the end moments M as a. function of b/a. Similar to the previous case, as $b/a\pm1$, all the stress curves converge into one point giving $h(b–a)/M](\sigma_r)_{max}=1,5$ which was established by equation (21). Notice that as the value of k increases, the magnitude of the delamination stress decreases. Figure 7 shows the dimensionless radial distance $[(r_m/a)–1]/[(b/a)–1]$ of $(\sigma')_{max}$ point measured from the inner boundary of the curved bar plotted as a function of *bla.* The effect of anisotropy turned out to be very small and could be neglected in the region $1<b/a<1,7$. As *bla* increases (that is, as the wall of the curved bar becomes thicker), the location of $(\sigma')_{max}$ moved inwardly away from the middle surface with a slower rate as compared with figure.

ISSN 2076-2429 (print)
ISSN 2223-3814 (on line)

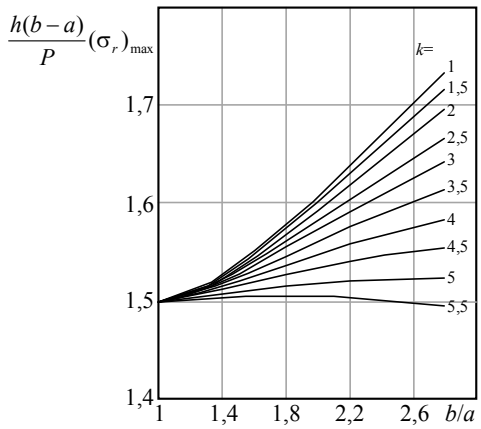

Fig. 6. Plots of delamination stress $(\sigma_r)_{max}$ As function of a/b for different valves of k

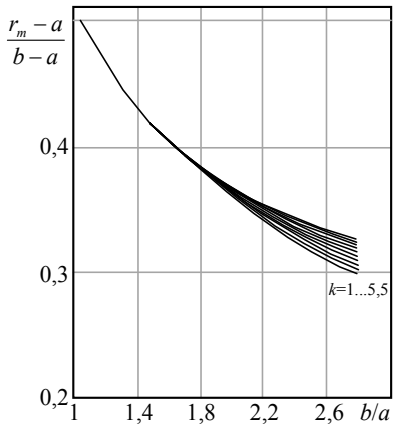

Fig. 7. Plots of location of stress $(\sigma_r)_{max}$ As function of a/b for different valves of k

Conclusion

In this paper it is studied the effect of tangential coordinate changes of the stress state of the semi-circular bar made of a composite material and consisting of many layers as well as it is investigated the relation between maximum peak radial stresses with the ratio of outer/to inner diameters at the different values of anisotropic parameters. The effect of anisotropy on the location of peak delamination stress was found to be small. The issues of stress state study indicated that change of tangential coordinate angle, the maximum value of radial stress is when the value of the tangential coordinate angle is equal to the ninetieth degree under the influence of forces and moments. But the maximum value for the tangential stress under the influence of forces is when the value of the tangential coordinate angle is equal to the ninetieth degree but maximum tangential stress under the influence of moment is when tangential coordinate is equal to zero and hundred eighty degree. The maximum shear stress is when tangential coordinate equal hundred eighty degree.

References

1. Reddy, J.N. Mechanics of Laminated Composite Plates and Shells — Theory and Analysis / J.N. Reddy. — CRC Press, 2003.
2. Chan, W.S., Demirhan, K.C. A Simple Closed-Form Solution of Bending Stiffness for Laminated Composite Tubes / W.S. Chan, K.C. Demirhan // J. of reinforced plastics and composites. — 2000. — Vol. 19, Issue 4. — P. 278 — 291.
3. Lin, C.Y., Chan, W.S. A Simple Analytical Method for Analyzing Laminated Composite Elliptical Tubes / C.Y. Lin, W.S. Chan // Proceedings of 17th technical conference, American Society of composites, October 2002.
4. Ren, J.G. Analysis of Laminated Circular Cylindrical Shells under Axisymmetric Loading / J.G. Ren // Composite Structures. — 1995. — Vol. 30, Issue 3. — P. 271 — 280.
5. Лехницкий, С.Г. Теория упругости анизотропного тела / С.Г. Лехницкий. — М.: Гостехиздат, 1977.
6. Hyer, M.W. Hydrostatic Response of Thick Laminated Composite Cylinders / M.W. Hyer // J. Reinforced Plastics and Composites. — 1988. — Vol. 7. — P. 321.
7. Roy, A.K. Design of Thick Composite Cylinders / A.K. Roy, S.W. Tsai // J. of Pressure Vessel Tech., Trans. of ASME. — 1988. — P. 110 — 255.
8. Ambartsumyan, S.A. Theory of Anisotropic Shells, NASA Technical Translation, NASA TTF – 118 / S.A. Ambartsumyan. — 1964.
9. Characterization of delamination onset and growth in a. composite laminate / T.K. O'Brien // Special Technical Testing Publication 775, American Society for Testing and Materials, 1982. — P. 140 — 167.

References

1. Reddy, J.N. Mechanics of Laminated Composite Plates and Shells — Theory and Analysis / J.N. Reddy. — CRC Press. 2003.
2. Chan, W.S., Demirhan, K.C. A Simple Closed-Form Solution of Bending Stiffness for Laminated Composite Tubes / W.S. Chan, K.C. Demirhan // J. of reinforced plastics and composites. — 2000. — Vol. 19, Issue 4. — P. 278 — 291.
3. Lin, C.Y., Chan, W.S. A Simple Analytical Method for Analyzing Laminated Composite Elliptical Tubes / C.Y. Lin, W.S. Chan // Proceedings of 17th technical conference, American Society of composites, October 2002.
4. Ren, J.G. Analysis of Laminated Circular Cylindrical Shells under Axisymmetric Loading / J.G. Ren // Composite Structures. — 1995. — Vol. 30, Issue 3. — P. 271 — 280.
5. Lekhnickiy, S.G. Teoriya uprugosti anizotropnogo tela [Theory of Anisotropic Elasticity] / S.G. Lekhnickiy. — Moscow, 1977.
6. Hyer, M.W. Hydrostatic Response of Thick Laminated Composite Cylinders / M.W. Hyer // J. Reinforced Plastics and Composites. — 1988. — Vol. 7. — P. 321.
7. Roy, A.K. Design of Thick Composite Cylinders / A.K. Roy, S.W. Tsai // J. of Pressure Vessel Tech., Trans. of ASME. — 1988. — P. 110 — 255.
8. Ambartsumyan, S.A. Theory of Anisotropic Shells, NASA Technical Translation, NASA TTF – 118 / S.A. Ambartsumyan. — 1964.
9. Characterization of delamination onset and growth in a composite laminate / T.K. O'Brien // Special Technical Testing Publication 775, American Society for Testing and Materials, 1982. — P. 140 — 167.

Reviewer Dr. techn. sciences, prof. of Odesa nat. polytechnic unit. Derevianchenko O.G.

Received November 27, 2011